

Free-space propagation of optical coherence lattices and periodicity reciprocity

Liyuan Ma and Sergey A. Ponomarenko*

Department of Electrical and Computer Engineering, Dalhousie University,
Halifax, NS, B3J 2X4 Canada

*serpo@dal.ca

Abstract: We examine paraxial propagation of recently introduced optical coherence lattices in free space and demonstrate a novel phenomenon of periodicity reciprocity between their intensity and coherence properties. The periodicity reciprocity arises because an aperiodic source intensity profile of an optical coherence lattice evolves into a lattice-like far-field profile, while the periodic spectral degree of coherence at the source becomes aperiodic on free-space propagation. We discuss how the discovered periodicity reciprocity can make optical coherence lattices attractive for robust free-space optical communications.

© 2015 Optical Society of America

OCIS codes: (030.0030) Coherence and statistical optics; (030.1640) Coherence; (030.4070) Modes; (050.1940) Diffraction.

References and links

1. J. Turunen and A. T. Friberg, "Propagation-Invariant Optical Fields," *Progress in Optics*, **54**, 1–88 (2010), ed. E. Wolf.
2. S. A. Ponomarenko and G. P. Agrawal, "Linear optical bullets," *Opt. Commun.* **261**, 1–4 (2006).
3. S. A. Ponomarenko, W. Huang, and M. Cada, "Dark and antidark diffraction-free beams," *Opt. Lett.* **32**, 2508–2510 (2007).
4. F. Gori, "Collett-Wolf sources and multimode lasers," *Opt. Commun.* **34**, 301–305 (1980).
5. A. Starikov and E. Wolf, "Coherent-mode representation of Gaussian Schell-model sources and their radiation fields," *J. Opt. Soc. Am.* **72**, 923–928 (1982).
6. R. Simon and N. Mukunda, "Twisted Gaussian Schell-model beams," *J. Opt. Soc. Am. A* **10**, 95–109 (1993).
7. S. A. Ponomarenko, "Twisted Gaussian Schell-model solitons," *Phys. Rev. E* **64**, 036618 (2001).
8. A. T. Friberg, E. Tervonen, and J. Turunen, "Interpretation and experimental demonstration of twisted Gaussian Schell-model beams," *J. Opt. Soc. Am. A* **11**, 1818–1826 (1994).
9. S. A. Ponomarenko, "A class of partially coherent beams carrying optical vortices," *J. Opt. Soc. Am. A* **18**, 150–156 (2001).
10. G. V. Bogatyryova, C. V. Fel'de, P. V. Polyanskii, S. A. Ponomarenko, M. S. Soskin, and E. Wolf, "Partially coherent separable vortex beams," *Opt. Lett.* **28**, 878–880 (2003).
11. F. Gori, "Mode propagation of the fields generated by Collett-Wolf Schell-model sources," *Opt. Commun.* **46**, 149–154 (1983).
12. L. Mandel and E. Wolf, *Optical Coherence and Quantum Optics*, (Cambridge University Press, 1997).
13. F. Gori, G. Guattari, and C. Padovani, "Modal expansion for J_0 -correlated Schell-model sources," *Opt. Commun.* **64**, 311–316 (1987).
14. C. Palma, R. Borghi, and C. Cincotti, "Beams originated by J_0 -correlated Schell-model sources," *Opt. Commun.* **125**, 113–121 (1996).
15. O. Korotkova, S. Sahin, and E. Shechepakina, "Multi-Gaussian Schell-model beams," *J. Opt. Soc. Am. A* **29**, 2159–2164 (2012).
16. C. Liang, X. Liu, F. Wang, Y. Cai, and O. Korotkova, "Cosine-Gaussian-correlated Schell-model beams with rectangular symmetry," *Opt. Lett.* **39**, 769–772 (2014).

17. H. Lajunen and T. Saastamoinen, "Propagation characteristics of partially coherent beams with spatially varying correlations," *Opt. Lett.* **36**, 4104–4106 (2011).
18. H. T. Eyyuboglu and Y. Baykal, "Transmittance of partially coherent cosh-Gaussian, cos-Gaussian, and annular beams through turbulence," *Opt. Commun.* **278** 17–22 (2007).
19. G. Zhou and X. Chu, "Propagation of partially coherent cosine-Gaussian beam through an ABCD optical system in turbulent atmosphere," *Opt. Express* **17** 10529–10534 (2009).
20. Z. Mei and O. Korotkova, "Propagation of cosine-Gaussian-correlated Schell-model beams in atmospheric turbulence," *Opt. Express* **21** 17512–17519 (2013).
21. F. Gori, "Lau effect and coherence theory," *Opt. Commun.* **31**, 4–8 (1983).
22. L. Liu, "Partially coherent diffraction effect between Lau and Talbot effects," *J. Opt. Soc. Am. A* **5**, 1709–1716 (1988).
23. A. W. Lohman and J. Ojeda-Castaneda, "Spatial periodicities in partially coherent fields," *Opt. Acta: Int. J. Opt.* **30**, 475–479 (1983).
24. G. Indebetouw, "Propagation of spatially periodic wavefields," *Opt. Acta: Int. J. Opt.*, **31**, 4–8 (1984).
25. J. Turunen, A. Vasara, and A. T. Friberg, "Propagation invariance and self-imaging in variable-coherence optics," *J. Opt. Soc. Am. A* **8**, 282–289 (1991).
26. S. Teng, L. Liu, J. Zu, Z. Luan, and L. Liu, "Uniform theory of the Talbot effect with partially coherent light illumination," *J. Opt. Soc. Am. A* **20**, 1747–1754 (2003).
27. M. Santarsiero, J. C. G. de Sande, G. Piquero, and F. Gori, "Coherence-polarization properties of fields radiated from transversely periodic electromagnetic sources," *J. Opt.* **15**, 055701 (2013).
28. L. Ma and S. A. Ponomarenko, "Optical coherence gratings and lattices," *Opt. Lett.* **39**(23), 6656–6659 (2011).
29. S. A. Ponomarenko, "Complex Gaussian representation of statistical pulses," *Opt. Express* **19**, 17086–17091 (2011).
30. S. A. Ponomarenko, and E. Wolf, "Coherence properties of light in Young's interference pattern formed with partially coherent light," *Opt. Commun.* **170**, 1–8 (1999).
31. S. A. Ponomarenko, and E. Wolf, "The spectral degree of coherence of fully spatially coherent electromagnetic beams," *Opt. Commun.*, **227**, 73–74 (2003).
32. E. Wolf, *Introduction to the Theory of Coherence and Polarization of Light* (Cambridge Univ. Press, 2007).

1. Introduction

Owing to the immunity of partially coherent beams to speckle formation in optical imaging and their robustness to natural media fluctuations, research into optical communications with partially coherent light has recently enjoyed a renaissance. In particular, the potential of propagation-invariant (diffraction-free) coherent and partially coherent beams and pulsed beams for distortion-less free-space information/image transfer applications has been recognized [1, 2]. Moreover, special classes of diffraction-free partially coherent beams, such as dark diffraction-free beams [3], can serve as versatile optical traps for neutral nano-particles or even atoms. Shape-invariant (self-similar) partially coherent beams can also be useful in free-space speckle-free image transfer and free-space optical communications. Several prominent classes of self-similar partially coherent beams have been discovered to date, including Gaussian Schell-model [4, 5], and twisted Gaussian Schell-model [6–8] beams. By the same token, partially coherent modified-Bessel vortex beams [9], separable vortex beams [10] as well as some others [11] are shape invariant because they admit a coherent-mode decomposition [12] in terms of self-similar Laguerre-Gaussian [9, 10] or Hermite-Gaussian [11] modes.

Although non-shape-invariant partially coherent beams are fairly useless for optical communication applications, they can possess desirable attributes for far-field coherence or radiation pattern generation on demand. For instance, while J_0 -correlated partially coherent beams have drastically evolving coherence properties on free-space propagation [13, 14], various families of multi-Gaussian Schell-model beams can either form a flat-top radiation pattern [15] or split on propagation [16]. On the other hand, non-uniformly correlated Gaussian beams can have their peak intensity positions shift upon free-space propagation [17]. Some non-shape-invariant partially coherent beams were shown to form stable structures on short-distance propagation through the turbulent atmosphere [18–20].

Partially coherent beams with periodic cross-spectral densities present yet another important

class. The significance of such beams for imaging is revealed by the existence of Lau [21, 22] and Talbot [22–27] self-imaging effects for partially coherent light. In the first instance, self-imaging arises on paraxial propagation of light generated by completely incoherent sources with periodic intensity profiles. In the second instance, though, the periodicity of scalar cross-spectral densities [22, 23, 25, 26] or cross-spectral density tensors [27] for polarized or partially polarized sources, respectively, is required for self-imaging. Lately, a new class of partially coherent beams, optical coherence lattices (OCL), was introduced [28] using recently developed complex Gaussian representation (CGR) of statistical pulses and beams [29]. The newly discovered OCLs have aperiodic (Gaussian) intensity profiles and statistically homogeneous, periodic coherence properties, precluding Talbot self-imaging in free space. The natural question then arises: Can OCLs be useful for optical imaging, communications, or information transfer?

To address this issue, we examine free-space evolution properties of OCLs in this work. In particular, we explore how the intensity profile and spectral degree of coherence of an OCL change on paraxial propagation. We discover periodicity reciprocity between the intensity and coherence properties of optical coherence lattices. The new phenomenon manifests itself when an aperiodic, Gaussian intensity profile of the source evolves into a periodic array of lobes in the far zone, whereas the initially periodic spectral degree of coherence loses its periodicity on lattice propagation. Thus, the spectral degree of coherence periodicity at the source is transferred to the far-field intensity profile periodicity. We suggest that the phenomenon can find applications to robust free-space optical communications.

2. Problem formulation and preliminary analysis

We begin by recalling that the cross-spectral density of a beam field ensemble of recently discovered [28] optical coherence lattices at a pair of points (X_1, Y_1) and (X_2, Y_2) in the source plane can be expressed in a factorized form as

$$W(X_1, Y_1, X_2, Y_2, 0) = \prod_{s=X, Y} W(s_1, s_2, 0). \quad (1)$$

Here $X = x/\sigma_1$, $Y = y/\sigma_1$ are dimensionless Cartesian coordinates scaled to the rms width σ_1 of the source intensity profile and we will drop an irrelevant dependence of the cross-spectral density on frequency henceforth. Using the CGR of statistical beams [29], each factor $W(s_1, s_2, 0)$ can be expressed as

$$W(s_1, s_2, 0) = \int d^2\alpha \mathcal{P}_s(\alpha) \psi_\alpha^*(s_1, 0) \psi_\alpha(s_2, 0), \quad (2)$$

where \mathcal{P}_s is a nonnegative distribution function to guarantee non-negative definiteness of W and $d^2\alpha \equiv d(\text{Re } \alpha) d(\text{Im } \alpha)$. The pseudo-modes $\{\psi_\alpha(s, 0)\}$ are normalized,

$$\int ds \psi_\alpha^*(s, 0) \psi_\alpha(s, 0) = 1, \quad (3)$$

and form an over-complete set such that

$$\int d^2\alpha \psi_\alpha^*(s_1, 0) \psi_\alpha(s_2, 0) = \delta(s_1 - s_2). \quad (4)$$

In the OCL case [28], \mathcal{P}_s has the form

$$\mathcal{P}_s(\alpha) = \sum_{n_s} v_{n_s} \delta(\alpha - \alpha_{n_s}), \quad v_{n_s} \geq 0. \quad (5)$$

On substituting from Eq. (5) into (2), we arrive at a pseudo-mode expansion of $W(s_1, s_2, 0)$ in the form

$$W(s_1, s_2; 0) = \sum_{n_s} v_{n_s} \psi_{\alpha_{n_s}}^*(s_1, 0) \psi_{\alpha_{n_s}}(s_2, 0). \quad (6)$$

Here the mode weight distributions v_{n_s} specify the intensity associated with each mode and

$$\alpha_{n_s} = \frac{i\pi n_s}{a_s \sqrt{2}}, \quad (7)$$

where a_s is a (dimensionless) lattice constant in the s -direction and n_s is an integer. Each lattice pseudo-mode at the source can be expressed as

$$\psi_{\alpha_{n_s}}(s, 0) = \frac{e^{-(\text{Im} \alpha_{n_s})^2}}{\pi^{1/4}} \exp \left[-\frac{(s - \sqrt{2} \alpha_{n_s})^2}{2} \right]. \quad (8)$$

Next, let us recall that the cross-spectral density function of any partially coherent beam ensemble, propagating in free space, obeys the paraxial Wolf equation [12] which we re-write in the dimensionless form as

$$(2i\partial_Z + \nabla_{\perp 2}^2 - \nabla_{\perp 1}^2)W(X_1, Y_1, X_2, Y_2; Z) = 0. \quad (9)$$

The dimensionless propagation distance Z is naturally measured in Rayleigh range units z_R corresponding to a fully coherent source of the width σ_1 , $z_R = k\sigma_1^2$. Owing to the separability of Eq. (9) in the Cartesian coordinates, we can factorize W in any transverse plane $Z = \text{const} > 0$, i. e.,

$$W(X_1, Y_1, X_2, Y_2; Z) = \prod_{s=X, Y} W(s_1, s_2; Z), \quad (10)$$

where each factor can be expanded into the pseudo-modes as

$$W(s_1, s_2; Z) = \sum_{n_s} v_{n_s} \psi_{\alpha_{n_s}}^*(s_1, Z) \psi_{\alpha_{n_s}}(s_2, Z). \quad (11)$$

On substituting from Eqs. (10) and (11) and separating spatial variables in the transverse plane, we obtain a paraxial wave equation for each pseudo-mode as

$$(2i\partial_Z + \partial_s^2) \psi_{\alpha_{n_s}}(s, Z) = 0. \quad (12)$$

The appropriate solution to Eq.(12), subject to the initial condition at the source (8), can be obtained in the form

$$\psi_{\alpha_{n_s}}(s, Z) = \frac{e^{-(\text{Im} \alpha_{n_s})^2}}{\pi^{1/4} (1 + iZ)^{1/2}} \exp \left[-\frac{(s - \sqrt{2} \alpha_{n_s})^2}{2(1 + iZ)} \right]. \quad (13)$$

It follows from Eqs. (11) and (13), after elementary algebra, that the cross-spectral density of an optical lattice in any transverse plane $Z = \text{const}$ is given by Eq. (10) with

$$W(s_1, s_2; Z) = \frac{\exp \left[\frac{i(s_2^2 - s_1^2)}{2R(Z)} \right]}{\sqrt{\pi(1 + Z^2)}} \sum_{n_s} v_{n_s} \exp \left\{ \frac{i\pi n_s}{a_s} \left[\frac{s_2 - s_1}{\sigma^2(Z)} \right] \right\} \times \exp \left[-\frac{(s_1 - \pi n_s Z / a_s)^2 + (s_2 - \pi n_s Z / a_s)^2}{2\sigma^2(Z)} \right]. \quad (14)$$

In Eq. (14), $R(Z)$ and $\sigma(Z)$ are dimensionless radius of the curvature and rms width of the beam specified by the expressions

$$R(Z) = Z + 1/Z, \quad \sigma(Z) = \sqrt{1 + Z^2}. \quad (15)$$

In particular, the intensity profile of an OCL field can be found as

$$I(X, Y; Z) \equiv \prod_{s=X, Y} W(s, s; Z) = \frac{1}{\pi(1 + Z^2)} \prod_{s=X, Y} \sum_{n_s} v_{n_s} \exp \left[-\frac{(s - \pi n_s Z / a_s)^2}{\sigma^2(Z)} \right]. \quad (16)$$

A qualitative analysis of Eq. (16) indicates that an initially Gaussian beam starts branching out into a Gaussian lattice with the individual Gaussian node intensities decreasing in amplitude on propagation. Further, each Gaussian spreads and the distance between the adjacent lattice nodes increases. Over several Rayleigh distances, the rates of node width spreading and adjacent node separation are both proportional to Z . However, the latter exceeds the former, provided the lattice constant is small enough, $a_{X, Y} \leq \pi$. Under the circumstances, the structural stability of the lattice is no longer compromised. Otherwise, individual lattice nodes can start overlapping over a certain propagation distance, resulting in annihilation of the overall beam lattice structure. Hereafter, we will restrict our analysis to OCLs maintaining their lattice structure in the far-zone due to their potential for free-space optical communications.

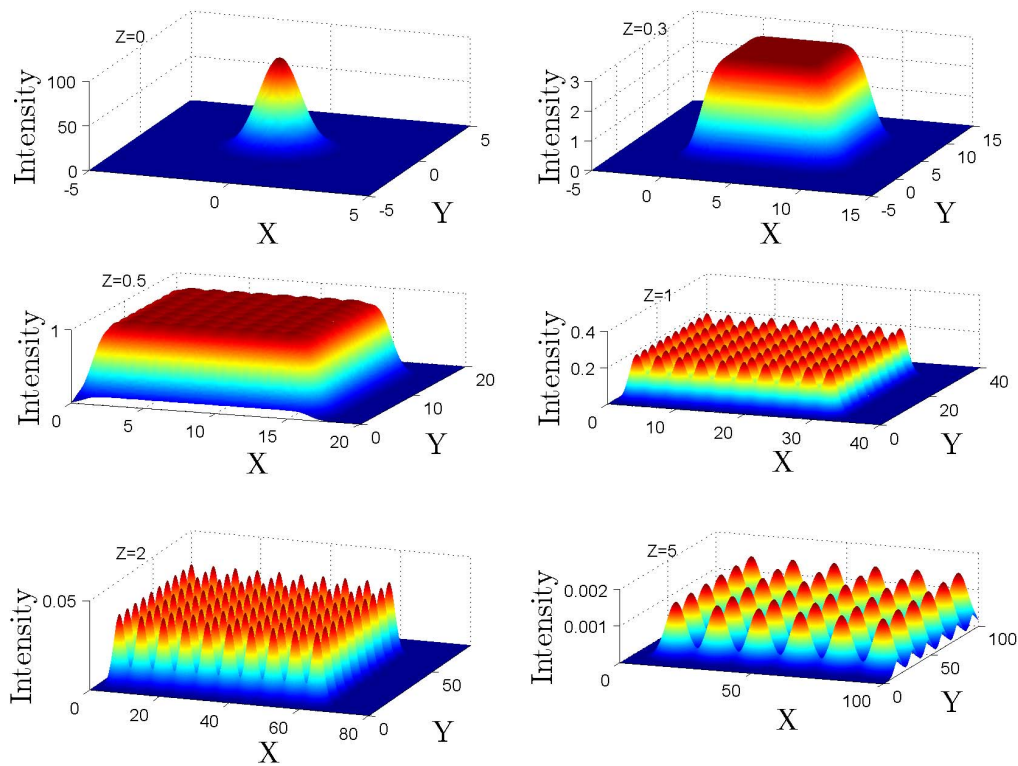


Fig. 1. Intensity profile (in arbitrary units) of a uniformly distributed OCL for several propagation distances Z . The lattice is composed of $N = 10$ lobes and the lattice constant is $a = 1$.

The spectral degree of coherence behavior follows from its definition [12, 30, 31]

$$\mu(X_1, Y_1, X_2, Y_2; Z) = \frac{W(X_1, Y_1, X_2, Y_2; Z)}{\sqrt{I(X_1, Y_1; Z)}\sqrt{I(X_2, Y_2; Z)}}, \quad (17)$$

together with Eqs. (10), (14) and (16). According to the van Cittert-Zernike theorem of the optical coherence theory [32], the lattices must become progressively more coherent on free-space propagation. In the following section, we illustrate the evolution of lattice intensity and spectral degree of coherence for several nontrivial cases.

3. The OCL intensity and spectral degree of coherence propagation in free space

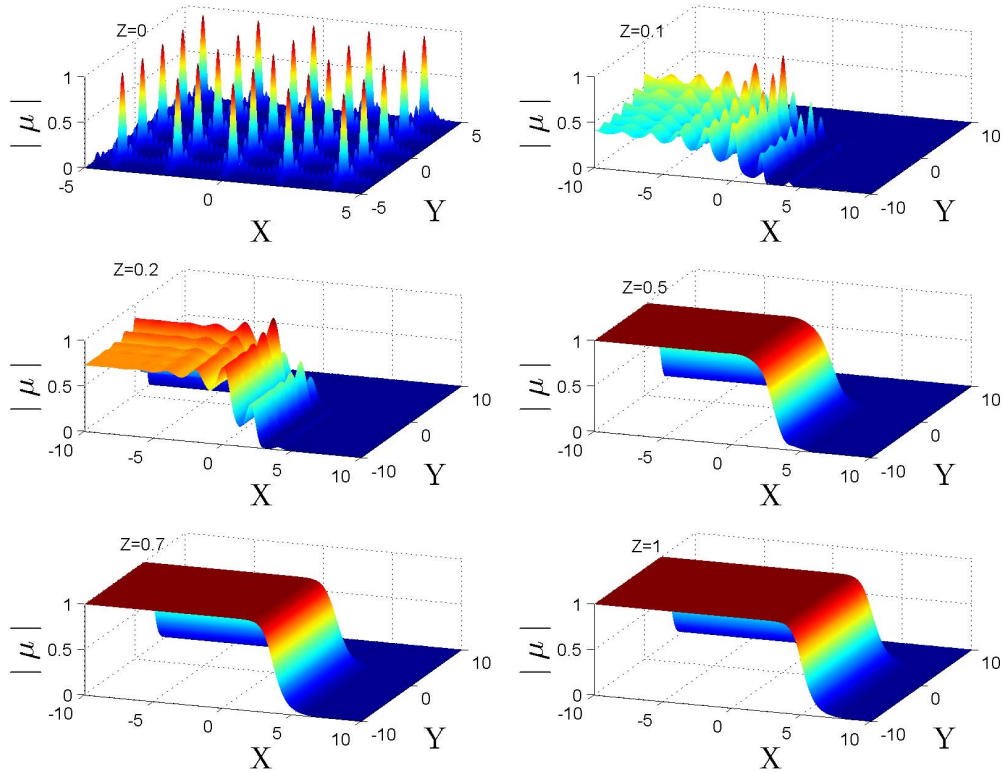


Fig. 2. Magnitude of the spectral degree of coherence of a uniformly distributed OCL for several propagation distances Z . The lattice is composed of $N = 10$ lobes and the lattice constant is $a = 1$.

We first consider an OCL composed of a finite number N of uniformly distributed complex Gaussian pseudo-modes such that

$$v_{n_x} = v_{n_y} = v_0 = \text{const}; \quad 0 \leq n_{X,Y} \leq N. \quad (18)$$

Under these conditions, the lattice intensity profile and spectral degree of coherence at the source can be evaluated in closed forms as [28]

$$I(X, Y, 0) \propto e^{-(X^2+Y^2)}, \quad (19)$$

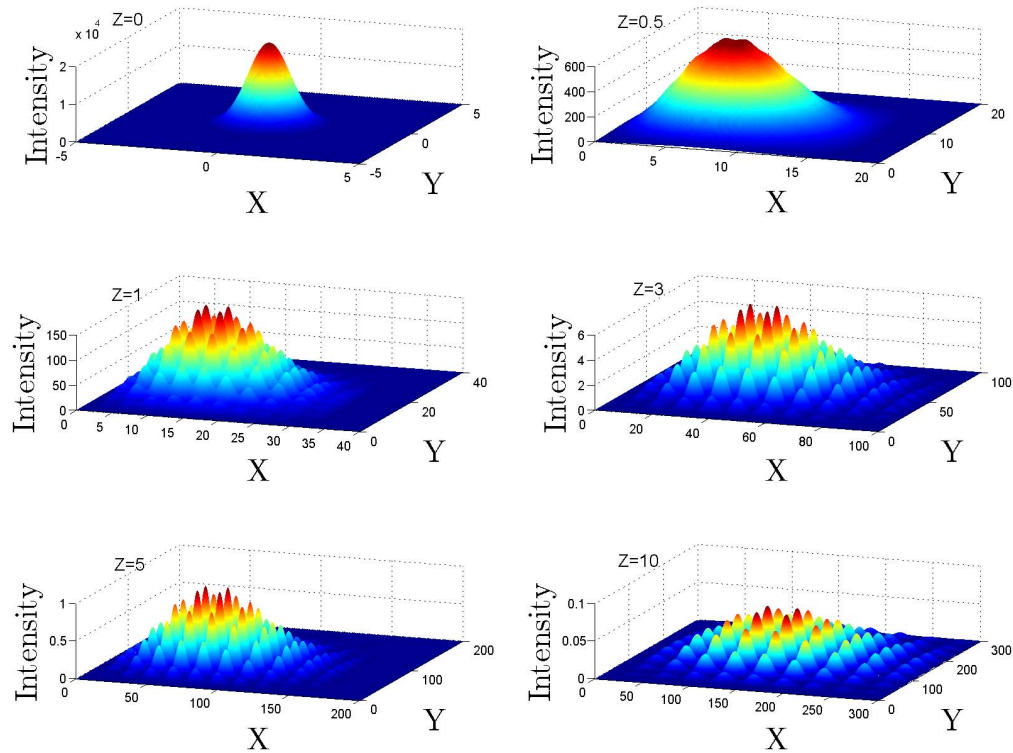


Fig. 3. Intensity profile (in arbitrary units) of a symmetric, non-uniformly distributed OCL for several propagation distances Z . The lattice constant is $a = 1$ and the weight distribution parameter is $\lambda = 5$.

up to an immaterial constant, and

$$|\mu(X_1, Y_1, X_2, Y_2; 0)| = \left| \frac{\sin \left[\frac{\pi N}{2a} (X_2 - X_1) \right] \sin \left[\frac{\pi N}{2a} (Y_2 - Y_1) \right]}{N^2 \sin \left[\frac{\pi}{2a} (X_2 - X_1) \right] \sin \left[\frac{\pi}{2a} (Y_2 - Y_1) \right]} \right|, \quad (20)$$

respectively. In deriving Eq. (20) we assumed, for simplicity, that the lattice constants in the X - and Y -directions are the same, $a_X = a_Y = a$.

Let us now display the behavior of the intensity and magnitude of the spectral degree of coherence of the lattice on its evolution with Z according to Eqs. (14) through (17). The intensity evolution is exhibited in Fig. 1, while the modulus of the spectral degree of coherence is shown in Fig. 2.

As can be inferred from Fig. 1, an originally aperiodic in intensity Gaussian beam forms a lattice on propagation. In accord with the above qualitative analysis after the intensity lattice has been formed, the lattice structure of the OCL remains intact, provided the lattice constant is not too large. The subsequent propagation into the far zone causes the lattice to expand and the individual node intensity maxima to decrease. The more-or-less stable lattice structure is formed over the Rayleigh range.

A quick look at Fig. 2 prompts the conclusion that the lattice structure of the source degree of coherence is destroyed on propagation, yielding an aperiodic spectral degree of coherence with the portion of the beam having $|\mu| = 1$ gradually increasing on propagation. Thus, the

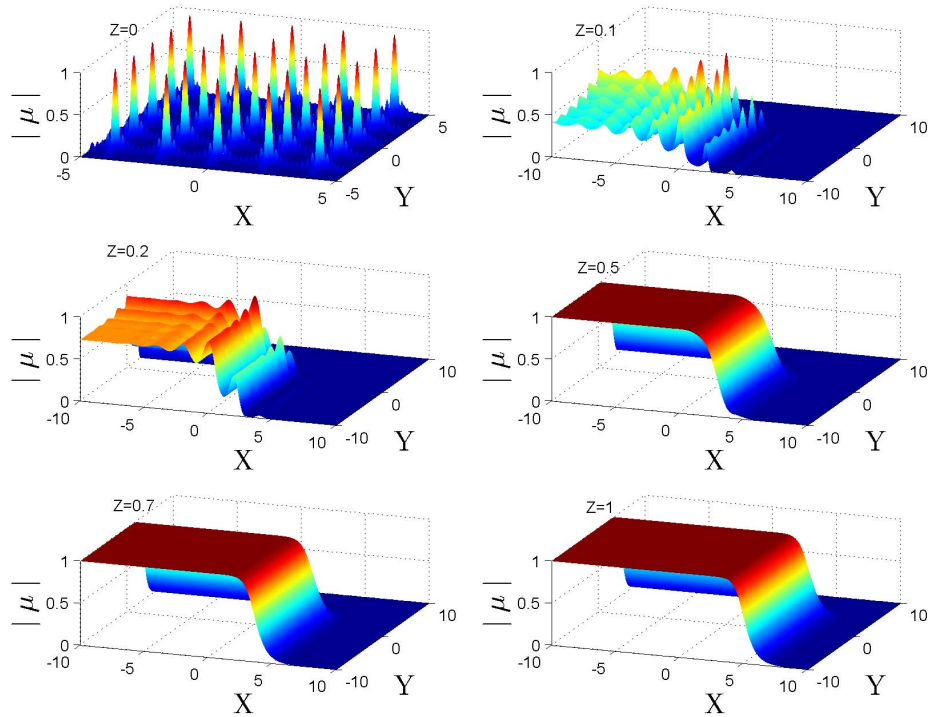


Fig. 4. Magnitude of the spectral degree of coherence of a symmetric, non-uniformly distributed OCL for several propagation distances Z . The lattice constant is $a = 1$ and the weight distribution parameter is $\lambda = 5$.

OCLs become progressively more coherent in agreement with the van Cittert-Zernike theorem. More instructively, however, we observe a curious reciprocity between the periodicity of OCL intensity and spectral degree of coherence. Indeed, while each lattice source has an aperiodic (Gaussian) intensity profile and a periodic spectral degree of coherence, a periodic intensity profile and aperiodic spectral degree of coherence emerge in the far zone of the source. We can conclude that, at least for uniformly distributed OCLs, the periodicity is transferred from the degree of coherence at the source to the far-field intensity.

To determine whether the discovered periodicity reciprocity is generic to OCLs, we will examine non-uniformly distributed OCL propagation. To this end, we consider an OCL with a nonuniform distribution of pseudo-modes as

$$v_{n_s} = \mathcal{A} \frac{\lambda_s^{n_s}}{n_s!}; \quad n_s \geq 0, \quad (21)$$

where \mathcal{A} is a positive constant. The corresponding source intensity is again Gaussian and the spectral degree of coherence at the source can be inferred from the Eqs. (14) through (17) as well as (21) such that

$$|\mu(X_1, Y_1, X_2, Y_2; 0)| = \exp \left\{ -2 \sum_{s=X,Y} \lambda_s \sin^2 \left[\frac{\pi(s_2 - s_1)}{2a_s} \right] \right\}. \quad (22)$$

We can then display the nonuniform OCL intensity and spectral degree of coherence behavior

in Figs. 3 and 4. We assume, for simplicity, that the lattices are symmetric with $a_X = a_Y = a$ and identically distributed along the X - and Y -axes such that $\lambda_X = \lambda_Y = \lambda$.

Figures 3 and 4 reveal the same key trends as do Figs. 1 and 2. Namely, the initially aperiodic source intensity profile gives rise to a periodic lattice and the initially periodic source spectral degree of coherence evolves into an aperiodic one. Thus, periodicity reciprocity is confirmed for non-uniformly distributed lattices as well and hence it appears to be a generic property of discovered OCLs. The only qualitative difference in the evolution of nonuniform from uniform OCLs, which is manifest on comparing Figs. 1 and 3, appears to be the intensity profile modulation of the former caused by a nonuniform distribution of their pseudo-modes.

4. Conclusions

In this work, we have explored the intensity and spectral degree of coherence evolution of recently introduced optical coherence lattices. We have shown that while an aperiodic source intensity profile of an OCL—which always happens to be Gaussian—develops spatial periodicity on paraxial propagation in free space, the initially lattice-like spectral degree of coherence loses its spatial periodicity on OCL propagation. Thus, the OCL periodicity has a reciprocity property: coherence-periodic OCLs at the source give rise to intensity-periodic far-field patterns. The discovered OCL periodicity reciprocity is shown to be generic for OCLs and it can be utilized in robust free-space optical communications. Indeed, specific information, encoded in an OCL via the periodicity of its spectral degree of coherence at the source, can be transmitted through a free-space link. The periodicity reciprocity of OCLs ensures that the encoded information is contained in the OCL far-field intensity pattern. The information can then be decoded by simply interrogating the OCL far-field intensity profile at the receiver.